Palenzonaite, berzeliite, and manganberzeliite: $(As^{5+},V^{5+},Si^{4+})O_4$ tetrahedra in garnet structures

M. Nagashima[1,*] and T. Armbruster[2]

[1] Graduate School of Science and Engineering, Yamaguchi University, Yoshida 1677-1, Yamaguchi 753-8512, Japan

[2] Mineralogical Crystallography, Institute of Geological Sciences, University of Bern, Freiestrasse 3, CH-3012 Bern, Switzerland

ABSTRACT

Schäferite, $NaCa_2Mg_2(V^{5+}O_4)_3$; palenzonaite, $NaCa_2Mn_2^{2+}(V^{5+}O_4)_3$; berzeliite, $NaCa_2Mg_2(As^{5+}O_4)_3$; and manganberzeliite, $NaCa_2Mn_2^{2+}(As^{5+}O_4)_3$, are cubic minerals with garnet structures (space group $Ia\bar{3}d$) in which tetrahedrally coordinated V^{5+} and/or As^{5+} at the Z site are charge balanced by disordered Na^+ and Ca^{2+} at the X site, and divalent Mg^{2+} and Mn^{2+} cations at the octahedrally coordinated Y site. The crystal chemistry of palenzonaite (from the Molinello and Gambatesa mines, Italy, and the Fianel mine, Switzerland), berzeliite (from Långban, Sweden, and Montaldo, Italy), and manganberzeliite (from Varenche, Italy, and the Gozaisho mine, Japan) were studied by electron microprobe analysis and single-crystal X-ray diffraction methods. Structure refinements converged to R_1 values of 1.36–2.42%. The tetrahedral site in these garnet structures is mainly occupied by pentavalent As^{5+} or V^{5+} (only up to about 20% randomly distributed Si^{4+} is present). Charge balance is maintained by variations in the Ca/Na ratio at the X site. Heterovalent substitution ($Na^+ \leftrightarrow Ca^{2+}$) at the distorted square antiprism X site in vanadate- and arsenate-bearing garnets allows full occupancy of the octahedral Y site by divalent cations (primarily Mg^{2+} and Mn^{2+}). There is a positive correlation between the <Z–O> and <Y–O> bond lengths and the mean ionic radii of the substituent elements, but there is no correlation between the <X–O> bond length and the variable Na/Ca site occupancy. The ionic radii of octahedrally coordinated Mg^{2+} and Mn^{2+} are such that the shared octahedral–dodecahedral edges are similar in length to the unshared octahedral edges, which is a measure of lattice distortion in garnet structures.

Introduction

The general formula for minerals with a garnet structure can be written $X_3Y_2(ZO_4)_3$. In the well known rock-forming silicate garnets, the X and Y sites are occupied by divalent and trivalent cations, respectively. A few non-silicate minerals including schäferite, ideally $NaCa_2Mg_2(V^{5+}O_4)_3$; palenzonaite, ideally $NaCa_2Mn_2^{2+}(V^{5+}O_4)_3$; berzeliite, ideally $NaCa_2Mg_2(As^{5+}O_4)_3$; and manganberzeliite, ideally $NaCa_2Mn_2^{2+}(As^{5+}O_4)_3$, have garnet structures. These vanadates and arsenates contain variable amounts of V^{5+}, As^{5+}, and Si^{4+} at the tetrahedral Z site. Due to their rarity, compositional heterogeneity and small crystal size, the structures of these minerals have not been studied in detail. However, the structure and properties of synthetic vanadate and arsenate garnets have been the subject of significant research (e.g. Bayer, 1965; Ito, 1968; Dukhovskaya and Mill, 1974; Schwarz and Schmidt, 1972, 1975; Nakatsuka *et al.*, 2003, 2004*a,b*; Iishi and Ikuta, 2006). In the vanadate

* E-mail: nagashim@yamaguchi-u.ac.jp

and arsenate garnets studied here, the eight-coordinated X site contains Na^+ and Ca^{2+} and the octahedrally coordinated Y site contains either Mn^{2+} or Mg^{2+}.

Palenzonaite was first described as thin veinlets in Mn-bearing calcite with braunite, cutting black manganese ore at the Molinello mine, Val Graveglia, Liguria, Italy (Basso, 1987). It also occurs with rare and unusual Mn arsenates, vanadates and silicates at several metamorphic Mn deposits in northern Italy and Switzerland (Brugger, 1995; Barresi et al., 2005, Roth and Meisser, 2011).

The only known locality for schäferite is the Bellberg volcano in the Eifel district, Germany, where it was found in a small cavity in a silicate xenolith in leucite tephrite lava (Krause et al., 1999).

Manganberzeliite has recently been reported from Varenche, and berzeliite from the Montaldo mine in same district where palenzonaite occurs (Barresi et al., 2005; Piccoli et al., 2007). Berzeliite and manganberzeliite are among the most common arsenates in skarn manganese ores at Långban, Sweden (Blix and Wickman, 1959; Holtstam and Langhof, 1999). Manganberzeliite also occurs as granular veinlets cutting the franklinite-willemite ore at Franklin, New Jersey (Frondel and Ito, 1963) and as veinlets with rhodonite, Mn(II)-bearing aegirine and rhodochrosite cutting black manganese ore consisting of braunite and hausmannite at the Gozaisho mine, Fukushima, Japan (Matsubara, 1975). Syntheses at $450-480ºC$ and 150 MPa, show that berzeliite and manganberzeliite form a continuous solid-solution, and their unit-cell parameters vary linearly with Mg/Mn ratio (Ito, 1968).

In this study, the crystal chemistry of three natural palenzonaite, two berzeliite, and two manganberzeliite specimens are reported. The experimental methods used were electron microprobe analysis (EMPA) and single-crystal X-ray diffraction. Variations of $(As^{5+}, V^{5+}, P^{5+}, Si^{4+})O_4$-tetrahedra are discussed for a systematic understanding of structural characteristics.

Experimental

Samples

Palenzonaite

One specimen of palenzonaite from each of the following localities was studied: (1) the Molinello mine (type locality; Basso, 1987); (2) the Gambatesa mine, Val Graveglia, Liguria, Italy;

and (3) the manganese ore deposit at Fianel, Val Ferrera, Graubünden, Switzerland (Brugger and Berlepsch, 1996). Palenzonaite occurs as small anhedral transparent brownish red crystals (less than 100 μm in diameter) associated with braunite and calcite at the Molinello and Gambatesa mines. It occurs as subhedral to euhedral dark red crystals with an approximately rhombododecahedral shape associated with quartz and yellow transparent nambulite at the Fianel mine (Nagashima and Armbruster, unpublished data).

Berzeliite

Specimens of berzeliite from (1) the Mn-rich skarn at Långban, Sweden (type locality; Blix and Wickman, 1959; Holtstam and Langhof, 1999); and (2) the Montaldo mine, Borgata Oberti, Piedmont, Italy (Piccoli et al., 2007) were studied. The transparent yellow anhedral berzeliite crystals from Långban are <0.4 mm in diameter, and associated with calcite and hausmannite. Transparent yellow anhedral berzeliite crystals from Montaldo vary in size from <10 μm (common) to 300 μm (rare) and are associated with quartz and hematite. Recently a $Ca-Na-Mn^{3+}$-arsenate with a formula $(Ca_{0.84}Na_{0.16})(Ca_{0.46}Na_{0.54})Mn_2^{3+}O(O,OH)(AsO_4)_2$ was reported from the Montaldo mine (Kolitsch, 2008).

Manganberzeliite

Specimens of manganberzeliite from (1) Varenche, Italy (Barresi et al., 2005), and (2) the Gozaisho mine, Fukushima, Japan (Matsubara, 1975) were studied. Manganberzeliite crystals from both localities are anhedral, yellowish orange and are slightly darker than berzeliite. They are <150 μm in size.

Chemical analysis (EMPA)

The compositions of palenzonaite, berzeliite and manganberzeliite were investigated using a JEOL JXA-8230 electron probe microanalyser at Yamaguchi University, Japan. The elements Si, P, V, As, Ti, Al, Cr, Fe, Mn, Mg, Ni, Pb, Ca, Sr, Ba, Na, K and Cu were analysed at an accelerating voltage of 15 kV, a beam current of 20 nA and a beam diameter of 1 μm. The following standards were used: natural wollastonite (Si, Ca), synthetic $KTiPO_4$ (P, K), synthetic $Ca_3(VO_4)_2$ (V), synthetic GaAs (As), synthetic rutile (Ti), synthetic corundum (Al), synthetic eskolaite (Cr), synthetic hematite (Fe), synthetic tephroite (Mn), synthetic

periclase (Mg), synthetic bunsenite (Ni), PbVGe-oxide (Pb), $SrBaNb_4O_{12}$ (Sr, Ba), natural albite (Na), natural orthoclase (K) and metallic copper (Cu). The Cr_2O_3 and CuO contents, which are not listed in Table 1, are negligible. The ZAF method was used for data correction. The severe overlap between the $MgK\alpha$ (1254 eV) and $AsL\alpha$ (1282 eV) peaks using a TAP analyser crystal were corrected with JEOL software.

Single-crystal structure analysis

Single-crystal X-ray diffraction data for palenzonaite, berzeliite and manganberzeliite were collected using Bruker SMART APEX II CCD diffractometers at the University of Bern, Switzerland and the Shimane University, Japan. The crystals were mounted on glass fibres and intensity data were measured at room temperature using graphite-monochromated $MoK\alpha$ radiation (λ = 0.71069 Å). Preliminary lattice parameters and an orientation matrix were obtained from twelve sets of frames and refined during the integration of the intensity data. Diffraction data were collected using ω scans at different φ settings (φ-ω scans) (Bruker, 1999). Data were processed using *SAINT* (Bruker, 1999). An empirical absorption correction using *SADABS* (Sheldrick, 1996) was applied. Structural refinement was performed using *SHELXL-97* (Sheldrick, 2008) and scattering factors for neutral atoms were employed. The Ca and Na present was assigned to the X site, Mn and/or Mg to the Y site, and Si, V and/or As to Z site. The Ca and Na site-occupancy was fixed based on the EMPA data. In some specimens, the Ca content was higher than expected due to Si substitution at the tetrahedral Z site: $^XCa + {}^ZSi^{4+} \leftrightarrow {}^XNa + {}^ZM^{5+}$. In the Si-bearing samples, the Si content was fixed on the basis of the EMPA results during the refinements. The high crystal quality of berzeliite and manganberzeliite led to signs of extinction and multiple diffraction and an extinction correction was made. The diffraction data did not indicate any lowering of symmetry from cubic $Ia\bar{3}d$.

Results

Chemical composition

The mean compositions of the studied specimens, normalized to eight cations, are listed in Table 1; total Mn, Fe, V and As are reported as MnO, FeO, V_2O_5 and As_2O_5, respectively. With the exception of palenzonaite from the Molinello mine, the total (Si + As + V + P) content based on the average chemical composition sums to 2.94−3.00 atoms per formula unit (a.p.f.u.). In general, the As, V and P ions are pentavalent and occupy tetrahedral sites, however, the palenzonaite from Molinello may contain a small amount of V^{3+} as the total (Si + As + V + P) content is >3 a.p.f.u. and there is a deficiency in the number of octahedrally coordinated Y-site cations. Thus, the amount of tetrahedral V^{5+} in palenzonaite from Molinello is calculated as 3 − (Si + As + P), and excess V is assigned as octahedrally coordinated V^{3+}. The possible presence of trivalent arsenic was not considered: As^{3+} in regular octahedral coordination is not expected as the coordination of As^{3+} is governed by its lone electron pair. Palenzonaite from the three different localities can be divided into two compositional variants: the specimen from Fianel has a high arsenic content (1.21 a.p.f.u.) compared to the others (0.17 a.p.f.u.). The compositions of berzeliite from the two different localities are similar, but the FeO content of Montaldo berzeliite is higher. The V_2O_5 content of manganberzeliite in the specimen from Varenche (4.76 wt.% V_2O_5) is higher than that in the Gozaisho specimen (1.07 wt.% V_2O_5). In summary, Σ(Ca + Na + K) tends to be slightly higher and Σ(Si + As + V + P) lower than the ideal values. The homogeneity of each studied specimen was confirmed by backscattered electron imaging; chemical zonation is not significant.

Crystal-structure solution and refinement

Crystallographic data and refinement parameters are summarized in Table 2. The refined atom positions and anisotropic mean-square displacement parameters are listed in Tables 3 and 4. Interatomic distances and selected angles are listed in Table 5. The occupancies of the cation sites are summarized in Table 6. The crystal structure of palenzonaite is shown in Fig. 1. Structure refinements in this study converged to R_1 values of 1.36−2.42%. The observed mean electron densities are almost consistent with the calculated values based on the expected site occupancies derived from the average chemical compositions (Table 6).

Discussion

Variation of the unit-cell parameters and cation distributions

The unit-cell parameters of all of the palenzonaite specimens are similar to each other even though

TABLE 1a. Compositions of palenzonaite, berzeliite and manganberzelite.

| | Palenzonaite | | | | | | Berzeliite | | | | Manganberzelite | | | |
| | Molinello mine, Italy ($n = 24$) | | Gambatesa mine, Italy ($n = 8$) | | Fianel mine, Switzerland ($n = 12$) | | Långban, Sweden ($n = 27$) | | Montaldo mine, Italy ($n = 22$) | | Varenche, Italy ($n = 22$) | | Gozaisho mine, Japan ($n = 22$) | |
	Mean	SD	Mean	SD	Mean	SD	Mean	SD	Mean	SD	Mean	SD	Mean	SD
Oxide composition (wt.%)														
SiO_2	1.98	0.23	1.87	0.11	0.38	0.09	0.73	0.23	0.17	0.05	0.07	0.04	0.43	0.11
P_2O_5	0.00	0.01	0.03	0.07	0.00	0.01	0.25	0.09	0.05	0.03	0.01	0.02	0.00	0.00
V_2O_5	44.37	1.25	42.71	0.71	26.36	1.99	0.33	0.07	1.32	0.11	4.76	1.26	1.07	0.12
As_2O_5	3.44	0.36	3.49	0.68	23.68	2.01	57.40	0.70	57.73	0.67	49.94	1.75	52.99	0.38
TiO_2	0.04	0.07	0.03	0.05	0.04	0.05	0.03	0.04	0.10	0.10	0.01	0.02	0.05	0.05
Al_2O_3	0.02	0.03	0.04	0.06	0.03	0.04	0.00	0.00	0.00	0.00	0.01	0.02	0.01	0.01
FeO	0.04	0.06	0.08	0.13	0.13	0.19	0.06	0.06	1.52	0.28	0.02	0.02	0.06	0.05
MnO	23.20	1.50	25.25	0.85	23.79	1.02	3.51	0.32	1.24	0.16	18.26	1.34	20.86	0.29
MgO	0.02	0.03	0.02	0.03	0.32	0.13	11.69	0.30	12.26	0.29	2.93	1.04	1.12	0.15
NiO	0.08	0.12	0.10	0.10	0.15	0.15	0.03	0.03	0.03	0.04	0.02	0.03	0.01	0.02
PbO	0.20	0.16	0.13	0.15	0.75	0.31	0.05	0.05	0.02	0.02	0.00	0.00	0.00	0.00
CaO	22.38	0.30	22.13	0.55	19.49	0.37	20.63	0.24	19.43	0.28	18.44	0.38	18.21	0.21
SrO	0.01	0.02	0.00	0.00	0.04	0.07	0.00	0.00	0.00	0.00	0.00	0.01	0.00	0.00
BaO	0.08	0.10	0.06	0.15	0.06	0.10	0.00	0.00	0.00	0.00	0.00	0.01	0.02	0.02
Na_2O	4.30	0.52	4.43	0.35	5.16	0.33	4.82	0.11	5.50	0.15	5.19	0.18	5.05	0.10
K_2O	0.01	0.02	0.01	0.02	0.01	0.02	0.01	0.01	0.01	0.01	0.00	0.00	0.01	0.01
Total	100.16		100.39		100.37		99.53		99.37		99.69		99.90	
Composition on the basis of eight cations														
Si	0.19	0.02	0.17	0.01	0.04	0.01	0.07	0.02	0.02	0.00	0.01	0.00	0.04	0.01
P^{5+}	0.00	0.00	0.00	0.01	0.00	0.00	0.02	0.01	0.00	0.00	0.00	0.00	0.00	0.00
V^{5+}	2.75	0.09	2.63	0.05	1.69	0.12	0.02	0.00	0.08	0.01	0.32	0.09	0.07	0.01
As^{5+}	0.17	0.02	0.17	0.03	1.21	0.11	2.89	0.02	2.89	0.03	2.64	0.08	2.86	0.02
Ti	0.00	0.00	0.00	0.00	0.00	0.00	0.00	0.00	0.01	0.01	0.00	0.00	0.00	0.00
Al	0.00	0.00	0.00	0.01	0.00	0.00	0.00	0.00	0.00	0.00	0.00	0.00	0.00	0.00
Fe^{2+}	0.00	0.01	0.01	0.01	0.01	0.01	0.00	0.00	0.12	0.02	0.00	0.00	0.01	0.00
Mn^{2+}	1.84	0.08	1.99	0.05	1.96	0.07	0.29	0.02	0.10	0.01	1.57	0.12	1.82	0.02
Mg	0.00	0.00	0.00	0.00	0.05	0.02	1.68	0.03	1.75	0.04	0.44	0.15	0.17	0.02
Ni	0.01	0.01	0.01	0.01	0.01	0.01	0.00	0.00	0.00	0.00	0.00	0.00	0.00	0.00
Pb	0.00	0.00	0.00	0.00	0.02	0.01	0.00	0.00	0.00	0.00	0.00	0.00	0.00	0.00
Ca	2.25	0.06	2.21	0.06	2.03	0.03	2.13	0.02	2.00	0.03	2.00	0.04	2.01	0.02

	Molinello	Gambatesa	Fianel	Långban	Montaldo	Varenche	Gozaisho
Sr	0.00	0.00	0.00	0.00	0.00	0.00	0.00
Ba	0.00	0.01	0.00	0.00	0.00	0.00	0.00
Na	0.78	0.80	0.97	0.90	1.02	1.02	1.01
K	0.08	0.06	0.06	0.02	0.03	0.04	0.02
Total	8.00	8.00	8.00	8.00	8.00	8.00	8.00

TABLE 1*b*. Chemical formulae from the compositions listed in Table 1*a*.

Mineral	Locality	Formula
Palenzonaite	Molinello	$(Ca_{2.25}Na_{0.78})_{\Sigma 3.03}(Mn^{2+}_{1.84}Ni_{0.01}V_{0.01})_{\Sigma 1.96}(V^{5+}_{2.64}As_{0.17}Si_{0.19})_{\Sigma 3.00}O_{12.06}$
	Gambatesa	$(Ca_{2.21}Na_{0.80})_{\Sigma 3.01}(Mn^{2+}_{1.99}Fe^{2+}_{0.01}Ni_{0.01})_{\Sigma 2.01}(V^{5+}_{2.63}As^{5+}_{0.17}Si_{0.17})_{\Sigma 2.97}O_{11.96}$
	Fianel	$(Ca_{2.03}Na_{0.97})_{\Sigma 3.00}(Mn^{2+}_{1.96}Mg_{0.05}Pb_{0.02}Fe^{2+}_{0.01}Ni_{0.01})_{\Sigma 2.05}(V^{5+}_{1.69}As^{5+}_{1.21}Si_{0.04})_{\Sigma 2.94}O_{11.90}$
Berzeliite	Långban	$(Ca_{2.13}Na_{0.90})_{\Sigma 3.03}(Mg_{1.68}Mn^{2+}_{0.29})_{\Sigma 1.97}(As^{5+}_{2.89}Si_{0.07}V^{5+}_{0.02}P_{0.02})_{\Sigma 3.00}O_{12.02}$
	Montaldo	$(Ca_{2.00}Na_{1.02})_{\Sigma 3.02}(Mg_{1.75}Mn^{2+}_{0.10}Fe^{2+}_{0.12}Ti_{0.01})_{\Sigma 1.98}(As^{5+}_{2.89}Si_{0.02}V^{5+}_{0.08})_{\Sigma 2.99}O_{11.97}$
Manganberzeliite	Varenche	$(Ca_{2.00}Na_{1.02})_{\Sigma 2.01}(Mn^{2+}_{1.57}Mg_{0.44})_{\Sigma 2.01}(As^{5+}_{2.64}V^{5+}_{0.32}Si_{0.01})_{\Sigma 2.97}O_{11.94}$
	Gozaisho	$(Ca_{2.01}Na_{1.01})_{\Sigma 3.02}(Mn^{2+}_{1.82}Mg_{0.17}Fe^{2+}_{0.01})_{\Sigma 2.00}(As^{5+}_{2.86}V^{5+}_{0.07}Si_{0.04})_{\Sigma 2.97}O_{11.92}$

TABLE 2. Experimental details of the single-crystal X-ray diffraction analyses of palenzonaite, berzeliite and manganberzeliite.

Locality	Palenzonaite			Berzeliite		Manganberzeliite	
	Molinello mine	Gambatesa mine	Fianel mine	Långban	Montaldo mine	Varenche	Gozaisho mine
Crystal size (mm)	$0.02 \times 0.025 \times 0.035$	$0.045 \times 0.03 \times 0.01$	$0.035 \times 0.03 \times 0.02$	$0.30 \times 0.25 \times 0.07$	$0.20 \times 0.15 \times 0.07$	$0.08 \times 0.05 \times 0.04$	$0.135 \times 0.10 \times 0.02$
a (Å)	12.543(1)	12.5359(2)	12.5342(2)	12.3450(2)	12.3404(2)	12.4829(1)	12.4929(2)
V (Å^3)	1973.49(3)	1970.00(1)	1969.20(1)	1881.37(1)	1879.26(1)	1945.12(1)	1949.80(1)
D_{calc} (g cm^{-3})	3.77	3.78	3.93	4.06	4.00	4.15	4.22
θ_{min}(°)	4.0	4.0	4.0	4.0	4.0	4.0	4.0
θ_{max}(°)	30.3	36.3	30.0	36.3	36.3	36.0	36.0
μ (mm^{-1})	7.70	7.71	7.71	11.94	11.95	15.14	12.69
Collected refl.	3129	9095	6045	2909	4247	12,372	7808
Unique refl.	245	406	244	383	384	395	388
R_{int} (%)	4.98	4.04	5.53	2.12	1.91	4.19	2.57
R_s (%)	2.33	1.83	2.29	1.47	1.05	1.10	1.10
Index limits	$-13 < h < 10$ $-5 < k < 17$ $-17 < l < 12$	$-12 < h < 20$ $-14 < k < 20$ $-15 < l < 20$	$-17 < h < 16$ $-14 < k < 17$ $-17 < l < 17$	$-11 < h < 20$ $-18 < k < 10$ $-17 < l < 13$	$-18 < h < 15$ $-20 < k < 18$ $-20 < l < 19$	$-19 < h < 20$ $-19 < k < 19$ $-15 < l < 20$	$-20 < h < 20$ $-16 < k < 17$ $-20 < l < 19$
R_1 (%)	2.34	2.42	1.87	1.55	1.37	1.88	1.36
wR_2 (%)	6.17	6.05	4.39	3.90	3.47	4.29	3.28
Parameters	19	19	19	20	20	19	20
Weighting*	$w = 1/[\sigma^2(F_o^2) + (0.0263P)^2 + 2.74P]$	$w = 1/[\sigma^2(F_o^2) + (0.0273P)^2 + 0.27P]$	$w = 1/[\sigma^2(F_o^2) + (0.0141P)^2 + 2.79P]$	$w = 1/[\sigma^2(F_o^2) + (0.0179P)^2 + 0.92P]$	$w = 1/[\sigma^2(F_o^2) + (0.0167P)^2 + 0.54P]$	$w = 1/[\sigma^2(F_o^2) + (0.0182P)^2 + 0.92P]$	$w = 1/[\sigma^2(F_o^2) + (0.0120P)^2 + 1.62P]$
$\Delta\rho_{max}$ (e Å^{-3})	0.28	0.34	0.30	0.37	0.31	0.33	0.21
$\Delta\rho_{min}$ (e Å^{-3})	−0.59	−0.81	−0.36	−0.37	−0.52	−0.63	−0.27

* The weighting scheme is $w = 1/(\sigma(F_o^2) + (aP)^2 + bP)$, where $P = (Max(F_o^2) + 2F_c^2)/3$, and the parameters a and b are chosen to minimize the differences in the variances for reflections in different ranges of intensity and diffraction angle.

TABLE 3. Atom positions and isotropic temperature factors (Å^2) for palenzonaite, berzeliite and manganberzeliite.

		Palenzonaite			Berzeliite		Manganberzeliite	
		Molinello mine, Italy	Gambatesa mine, Italy	Fianel mine, Switzerland	Långban, Sweden	Montaldo mine, Italy	Varenche, Italy	Gozaisho mine, Japan
X	x/a	⅛	⅛	⅛	⅛	⅛	⅛	⅛
	y/a	0	0	0	0	0	0	0
	z/a	¼	¼	¼	¼	¼	¼	¼
	U_{eq}	0.0129(4)	0.0112(2)	0.0135(3)	0.0099(1)	0.0099(1)	0.0110(2)	0.0111(1)
Y	x/a	0	0	0	0	0	0	0
	y/a	0	0	0	0	0	0	0
	z/a	0	0	0	0	0	0	0
	U_{eq}	0.0111(3)	0.0095(2)	0.0122(2)	0.0081(3)	0.0084(2)	0.0093(2)	0.0095(1)
Z	x/a	⅜	⅜	⅜	⅜	⅜	⅜	⅜
	y/a	0	0	0	0	0	0	0
	z/a	¼	¼	¼	¼	¼	¼	¼
	U_{eq}	0.0074(3)	0.0064(1)	0.0085(2)	0.00506(8)	0.00525(7)	0.00675(9)	0.00637(7)
O	x/a	0.0329(1)	0.03924(7)	0.0397(1)	0.03903(6)	0.03893(5)	0.03963(8)	0.03973(6)
	y/a	0.0542(1)	0.05417(7)	0.0537(1)	0.05125(6)	0.05085(5)	0.05302(8)	0.05317(6)
	z/a	0.6584(1)	0.65829(6)	0.6588(1)	0.65664(6)	0.65608(5)	0.65865(8)	0.65912(6)
	U_{eq}	0.0132(5)	0.0118(2)	0.0150(4)	0.0091(2)	0.0088(2)	0.0112(2)	0.0110(2)

TABLE 4. Anisotropic displacement parameters (Å^2) for palenzonaite, berzeliite and manganberzeliite.

		Palenzonaite			Berzeliite		Manganberzeliite	
		Molinello mine, Italy	Gambatesa mine, Italy	Fianel mine, Switzerland	Långban, Sweden	Montaldo mine, Italy	Varenche, Italy	Gozaisho mine, Japan
X	U_{11}	0.0106(6)	0.0087(3)	0.0110(5)	0.0073(2)	0.00736(19)	0.0079(3)	0.0079(3)
	U_{22}	0.0141(4)	0.0124(2)	0.0147(3)	0.0116(16)	0.01113(15)	0.0125(2)	0.0125(2)
	U_{33}	0.0141(4)	0.0124(2)	0.0147(3)	0.0116(16)	0.01113(15)	0.0125(2)	0.0125(2)
	U_{23}	0.0016(4)	0.0016(2)	0.0019(3)	0.00208(16)	0.00158(13)	0.0021(2)	0.0021(2)
	U_{13}	0	0	0	0	0	0	0
	U_{12}	0	0	0	0	0	0	0
Y	U_{11}	0.0111(3)	0.0095(2)	0.0122(2)	0.0081(3)	0.0084(2)	0.0093(2)	0.0093(2)
	U_{22}	0.0111(3)	0.0095(2)	0.0122(2)	0.0081(3)	0.0084(2)	0.0093(2)	0.0093(2)
	U_{33}	0.0111(3)	0.0095(2)	0.0122(2)	0.0081(3)	0.0084(2)	0.0093(2)	0.0093(2)
	U_{23}	−0.0005(2)	−0.00060(9)	−0.0006(2)	−0.00047(14)	−0.00021(12)	−0.00038(10)	−0.00038(10)
	U_{13}	−0.0005(2)	−0.00060(9)	−0.0006(2)	−0.00047(14)	−0.00021(12)	−0.0004(1)	−0.00038(10)
	U_{12}	−0.0005(2)	−0.00060(9)	−0.0006(2)	−0.00047(14)	−0.00021(12)	−0.0004(1)	−0.00038(10)
Z	U_{11}	0.0076(5)	0.0056(2)	0.0079(3)	0.00499(11)	0.00504(9)	0.0065(1)	0.00645(14)
	U_{22}	0.0073(3)	0.0067(2)	0.0088(2)	0.00509(9)	0.00535(8)	0.0069(1)	0.00690(10)
	U_{33}	0.0073(3)	0.0067(2)	0.0088(2)	0.00509(9)	0.00535(8)	0.0069(1)	0.00690(10)
	U_{23}	0	0	0	0	0	0	0
	U_{13}	0	0	0	0	0	0	0
	U_{12}	0	0	0	0	0	0	0
O	U_{11}	0.0131(9)	0.0126(5)	0.0165(7)	0.0091(3)	0.0088(3)	0.0114(5)	0.0114(5)
	U_{22}	0.0143(10)	0.0126(4)	0.0153(7)	0.0104(3)	0.0100(3)	0.0126(4)	0.0126(4)
	U_{33}	0.0122(9)	0.0104(4)	0.0133(7)	0.0078(3)	0.0075(3)	0.0097(4)	0.0097(4)
	U_{23}	0.0008(7)	−0.0006(3)	0.0007(5)	0.0006(2)	0.0004(2)	0.0008(3)	0.0008(3)
	U_{13}	0.0002(8)	−0.0006(3)	−0.0007(5)	−0.0019(3)	−0.0017(2)	−0.0015(3)	−0.0015(3)
	U_{12}	0.0000(7)	−0.0001(3)	0.0005(5)	0.0013(2)	0.0010(2)	0.0012(3)	0.0012(3)

TABLE 5. Selected bond distances and angles for palenzonaite, berzeliite and manganberzeliite.

		Palenzonaite			Berzeliite		Manganberzeliite	
		Molinello mine, Italy	Gambatesa mine, Italy	Fianel mine, Switzerland	Långban, Sweden	Montaldo mine, Italy	Varenche, Italy	Gozaisho mine, Japan
$X1-O4$	$(\times 4)$	2.455(2)	2.4540(9)	2.454(1)	2.4143(8)	2.4144(7)	2.442(1)	2.4424(8)
$X2-O4$	$(\times 4)$	2.540(2)	2.5381(8)	2.546(1)	2.5308(7)	2.5332(6)	2.543(1)	2.5446(8)
$<X-O>$		2.498	2.496	2.500	2.4726	2.4738	2.493	2.4935
$<Y-O>$	$(\times 6)$	2.157(2)	2.1542(8)	2.160(1)	2.0908(7)	2.0819(6)	2.1459(9)	2.1538(7)
$<Z-O>$	$(\times 4)$	1.714(2)	1.7143(8)	1.704(1)	1.6897(7)	1.6927(6)	1.6953(9)	1.6927(7)
$O1-X2-O2$	$(\times 2)$	65.87(8)	65.93(4)	65.44(6)	65.99(3)	66.17(3)	65.37(4)	65.17(3)
$O1-X2-O4$	$(\times 4)$	74.91(8)	74.84(4)	75.15(6)	73.53(3)	73.17(3)	71.92(3)	71.74(3)
$O1-X2-O7$	$(\times 4)$	92.20(5)	92.23(2)	91.95(4)	91.93(2)	91.96(2)	91.85(2)	91.78(2)
$O4-X2-O6$	$(\times 4)$	71.61(6)	71.65(3)	71.68(5)	72.99(3)	73.26(2)	74.94(4)	75.22(3)
$O4-X2-O7$	$(\times 2)$	69.66(8)	69.64(4)	69.49(6)	69.80(3)	69.82(3)	69.58(4)	69.58(4)
$O7-X2-O8$	$(\times 2)$	113.70(8)	113.70(4)	113.94(6)	113.14(3)	113.01(3)	113.79(4)	113.89(3)
$O1-Y-O4$	$(\times 6)$	89.54(6)	89.54(3)	89.82(5)	89.83(3)	89.76(2)	90.05(4)	90.05(3)
$O1-Y-O5$	$(\times 6)$	90.46(6)	90.46(3)	90.18(5)	90.17(3)	90.24(2)	89.95(4)	89.95(3)
$O1-Z-O2$	$(\times 2)$	102.3(1)	102.33(6)	102.27(9)	102.18(5)	102.27(5)	102.10(7)	101.99(5)
$O1-Z-O3$	$(\times 4)$	113.19(6)	113.16(3)	113.19(5)	113.24(3)	113.19(3)	113.28(4)	113.33(3)
$\sigma_\theta(oct)^2$*		0.233	0.234	0.034	0.032	0.063	0.002	0.003

* Angular distortion parameters are as defined by Robinson et al. (1971); $\sigma_\theta(oct)^2 = \Sigma(\theta_i - 90°)/11$ where $\theta_i = O-M-O$ angle.

the specimen from Fianel is rich in arsenic compared to the others (Table 2). This is due to the similar mean ionic radii at the tetrahedral sites, which based on site occupancies are 0.353 Å for the crystals from Molinello and Gambatesa, and 0.351 Å for the crystal from Fianel. The unit-cell parameter reported by Basso (1987) for palenzonaite from the Molinello mine is similar to our experimental results, but those of synthetic $NaCa_2Mn^{2+}(V^{5+}O_4)_3$ (12.573 Å; Iishi and Ikuta, 2006; 12.568 Å Nakatsuka et al., 2004a) are slightly larger than the natural samples. The smaller cell dimensions in natural palenzonaite are related to partial substitution of tetrahedral As^{5+} (ionic radius, $r = 0.34$ Å) and Si^{4+} ($r = 0.26$ Å) for V^{5+} ($r = 0.36$ Å). The increase in the unit-cell size with increasing Mn^{2+} content in synthetic $NaCa_2Mg(As^{5+}O_4)_3$ (berzeliite) – $NaCa_2Mn^{2+}(As^{5+}O_4)_3$ (manganberzeliite) reported by (Ito, 1968), is also consistent with our results. The differences in the unit-cell parameters between palenzonaite (Mn^{2+} dominant at Y and V^{5+} dominant at Z) and manganberzeliite

(Mn^{2+} dominant at Y and As^{5+} dominant at Z) can be explained by the cation distribution at the tetrahedral site. The unit-cell parameters decrease in the order palenzonaite > manganberzeliite > berzeliite.

The sizes of the YO_6 octahedra and ZO_4 tetrahedra increase as the mean ionic radii of the central elements increase (Fig. 2a,b; $R^2 = 0.96$ for Y and 0.88 for Z). There is no correlation between the size of the XO_8 polyhedra and the mean ionic radius of the elements at X in our data despite reported increases in $<X-O>$ distances in silicate garnets with increasing mean ionic radius (Hawthorne, 1981). However, Na ($r = 1.18$ Å) and Ca ($r = 1.12$ Å) in eightfold coordination have similar ionic radii (Shannon, 1976) and the Ca/Na ratio in our samples only varies between 2.00 and 2.85, which corresponds to an increase of 1.136 to 1.140 Å in the mean ionic radius. The distorted square antiprism at X in berzeliite is smaller than those in palenzonaite and manganberzeliite (Fig. 2c). As a result of the low average charge at the X site, the XO_8 polyhedra in these garnet

TABLE 6. Site occupancies for palenzonaite, berzeliite and manganberzeliite.

	Site	Observed no. e$^-$	Site occupancy based on EMPA	Calculated no. e$^-$
Palenzonaite				
	X	17.60	$Ca_{0.74}Na_{0.26}$	17.66
Molinello mine, Italy	Y	24.73	$Mn^{2+}_{0.95}V^{3+}_{0.05}$	24.90
	Z	22.51	$V^{5+}_{0.88}As^{5+}_{0.06}Si_{0.06}$	21.86
	X	17.60	$Ca_{0.74}Na_{0.26}$	17.66
Gambatesa mine, Italy	Y	24.73	$Mn^{2+}_{1.00}$	25.00
	Z	22.93	$V^{5+}_{0.88}As^{5+}_{0.06}Si_{0.06}$	21.86
	X	17.09	$Ca_{0.68}Na_{0.32}$	17.12
Fianel mine, Switzerland	Y	24.20	$Mn^{2+}_{0.98}Mg_{0.02}$	24.74
	Z	27.33	$V^{5+}_{0.58}As^{5+}_{0.41}Si_{0.01}$	27.01
Berzeliite				
	X	17.30	$Ca_{0.70}Na_{0.30}$	17.30
Långban, Sweden	Y	13.55	$Mg_{0.86}Mn^{2+}_{0.14}$	13.10
	Z	31.82	$As^{5+}_{0.97}Si(+ P)_{0.03}$	32.43
	X	17.00	$Ca_{0.67}Na_{0.33}$	17.03
Montaldo mine, Italy	Y	13.57	$Mg_{0.89}Fe^{2+}_{0.06}Mn^{2+}_{0.05}$	13.49
	Z	32.58	$As^{5+}_{0.97}V^{5+}_{0.03}$	32.70
Manganberzeliite				
	X	17.00	$Ca_{0.67}Na_{0.33}$	17.03
Varenche, Italy	Y	22.11	$Mn^{2+}_{0.78}Mg_{0.22}$	22.14
	Z	31.48	$As^{5+}_{0.89}V^{5+}_{0.11}$	31.90
	X	17.00	$Ca_{0.67}Na_{0.33}$	17.03
Gozaisho mine, Japan	Y	23.03	$Mn^{2+}_{0.91}Mg_{0.09}$	23.83
	Z	31.78	$As^{5+}_{0.97}V^{5+}_{0.02}Si_{0.01}$	32.28

structures make soft links between more rigid octahedra (Y) and tetrahedra (Z), although an appropriate Na/Ca ratio at X is vital for charge balance. Thus, the volume of the XO_8 polyhedra is not governed by the cation distribution at X.

The $(As^{5+},V^{5+},P^{5+},Si^{4+})O_4$ tetrahedron

Several silicate minerals with $(As^{5+},V^{5+},P^{5+},Si^{4+})O_4$ tetrahedra have been reported (Nagashima and Armbruster, 2010, table 10). Such tetrahedral sites can be categorized by the number of bridging apices to other tetrahedral sites (Nagashima and Armbruster, 2010). The $(As^{5+},V^{5+},P^{5+},Si^{4+})O_4$ tetrahedra in vanadate−arsenate garnets, such as palenzonaite, berzeliite and manganberzeliite, are isolated. There is a positive correlation between <Z–O> and the mean ionic radii of the central atoms in the $(As,V,P,Si)O_4$ tetrahedral site ($R^2 = 0.87$ in Fig. 3).

The stoichiometry puzzle

Schäferite, palenzonaite, berzeliite and manganberzeliite are characterized by a combined substitution in which pentavalent cations in tetrahedral coordination at Z are charge balanced by an appropriate ratio of monovalent and divalent Na$^+$ and Ca^{2+} cations at X, and divalent octahedrally coordinated cations at Y. This observation poses the following question: why are there no minerals with the garnet structure with pentavalent cations at Z and trivalent cations at Y, in which charge balance is maintained by univalent Na at X? A potential example is $Na_3Al_2(PO_4)_3$. Bond-strength arguments can be ruled out as the only O position in the cubic garnet structure is bonded once to Z and Y and twice to X: $5/4 + 3/6 + 2 \times 1/8 = 2$.

Of the synthetic vanadate garnets (V^{5+} at Z), those with Na and Ca at the X site predominate (Bayer, 1965). All of the vanadate garnets synthesized by Bayer (1965) at 700 to 750ºC by

solid state reaction, with Ca/Na = 2/1 at X, contain divalent cations with ionic radii (Shannon, 1976) between 0.690 Å ($^{VI}Ni^{2+}$) and 0.745 Å ($^{VI}Co^{2+}$) at the Y site. Synthetic palenzonaite [$Ca_2NaMn_2(VO_4)_3$] single crystals ($^{VI}Mn^{2+}$ = 0.83 Å) have been grown (Nakatsuka et al., 2004a) from oxides by the floating zone technique. Thus, the radius of the divalent cations at Y in vanadate garnets is generally larger than that of the common octahedrally coordinated trivalent cations in silicate garnets [$r(^{VI}Al^{3+})$ = 0.535 Å, $r(^{VI}Fe^{3+})$ = 0.645 Å]. A second group of vanadate garnets listed by Bayer (1965) contain Ca at X and a 1:1 ratio of octahedrally coordinated Li^+ and M^{2+} (Mg, Co, Ni, Cu and Zn) at Y. As octahedrally coordinated Li has an ionic radius 0.76 Å (Shannon, 1976),

these vanadate garnets are also characterized by rather large mean octahedral radii.

Thilo (1941) reported the synthesis of $Na_3Al_2(PO_4)_3$ with a garnet structure at 500ºC from an Na_3PO_4 and AlP_4O melt. However, these results were questioned by Brunet et al. (2006) who synthesized the same compound at 17 GPa and 1400−1600°C. Garnet-structured $Na_3Al_2(PO_4)_3$ with a = 11.579(2) Å has an oxygen position at 0.046(1), 0.045(1), 0.658(1) derived from low quality Rietveld powder refinement (Brunet et al., 2006).

As all cation sites in the cubic $Ia\bar{3}d$ garnet structure are fixed at special positions, and all the $Z-O$ and $Y-O$ distances are symmetrically equivalent, the position of the oxygen atom can be calculated from the known cell dimension
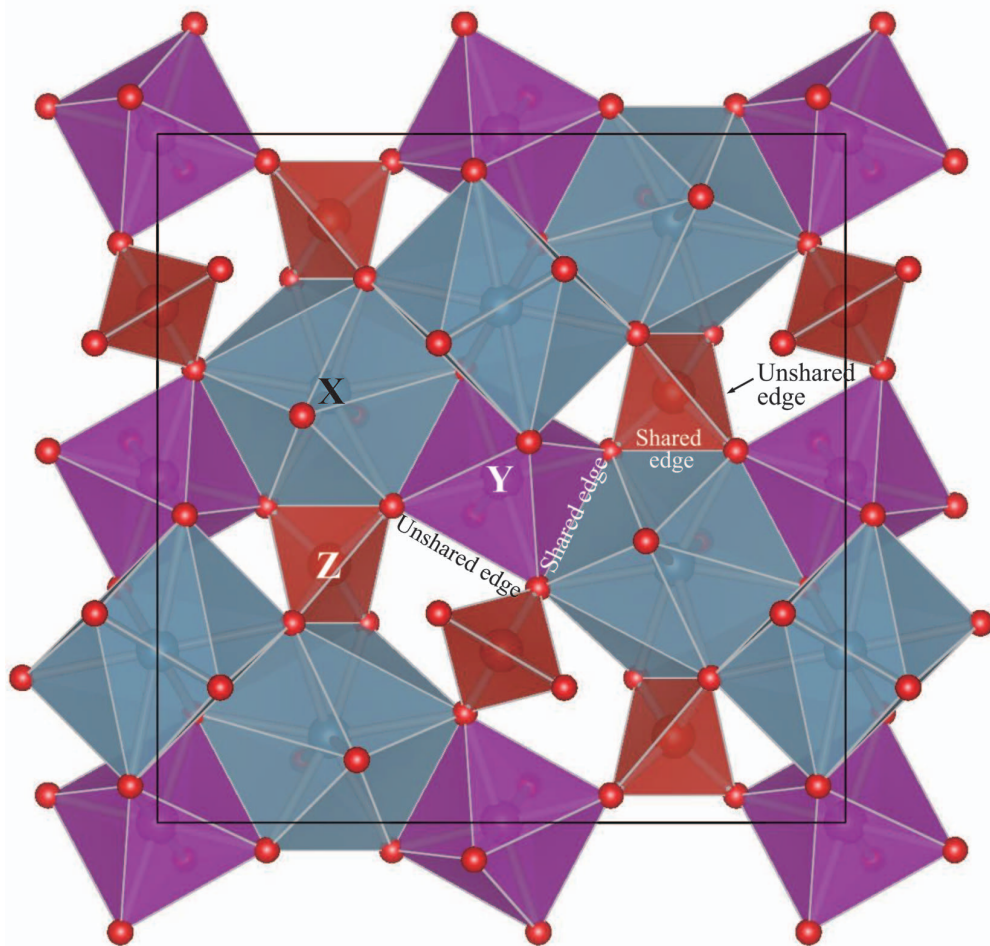

FIG. 1. The crystal structure of palenzonaite (drawn using VESTA; Momma and Izumi, 2008).

using P−O and Al−O bond lengths at Z and Y of P−O = 1.535 Å and Al−O = 1.921 Å, respectively. The calculated oxygen coordinates are 0.0441, 0.0428, 0.6541 which are close to the refined values (Table 7). The resulting Na−O distances at X are 2.305 and 2.477 Å, respectively. The corresponding garnet structure is characterized by large angular octahedral distortion (Table 7). The length of the edge shared between the octahedron (Y) and distorted square antiprism (X) is 2.818 Å, whereas the unshared octahedral edge is 2.612 Å in length. This difference in polyhedral edge length of ~0.2 Å is much larger than pyrope, the most distorted of the common silicate garnets, where the corresponding difference is ~−0.1 Å (Novak and Gibbs, 1971: the shared edge is shorter than the unshared octahedral edge).

Schwarz and Schmidt (1972) reported syntheses of two arsenates with garnet structures: $Na_3Cr_2(AsO_4)_3$ (a = 12.15 Å) between 850 and 900ºC and $Na_3Fe_2(AsO_4)_3$ (a = 12.22 Å) between 600 and 800ºC. Two vanadates: $Na_3Cr_2(VO_4)_3$ (a = 12.29 Å) and $Na_3Sc_2(VO_4)_3$ (a = 12.60 Å), synthesized at 550−600ºC and 750ºC, respectively, were subsequently described (Schwarz and Schmidt, 1975). In the absence of structural data, the oxygen position in the two Cr garnets with tetrahedral AsO_4 and VO_4 can be calculated assuming an octahedral Cr−O distance of 1.99 Å, As−O of 1.693 Å, and V−O of 1.72 Å (Table 7). The differences in the lengths of the shared and unshared octahedral edges are 0.046 Å (arsenate) and 0.068 Å (vanadate), which is considerably smaller than the high-pressure phosphate garnet (and similar to the silicate garnet grossular; Novak and Gibbs, 1971).

If the structures of the synthetic phosphate, arsenate and vanadate garnets which only contain Na at the X site are compared with the structures of schäferite, palenzonaite, berzeliite and manganberzeliite, it is clear that the synthetic phases are considerably more distorted than the minerals (Tables 5 and 7). The O−O distances of
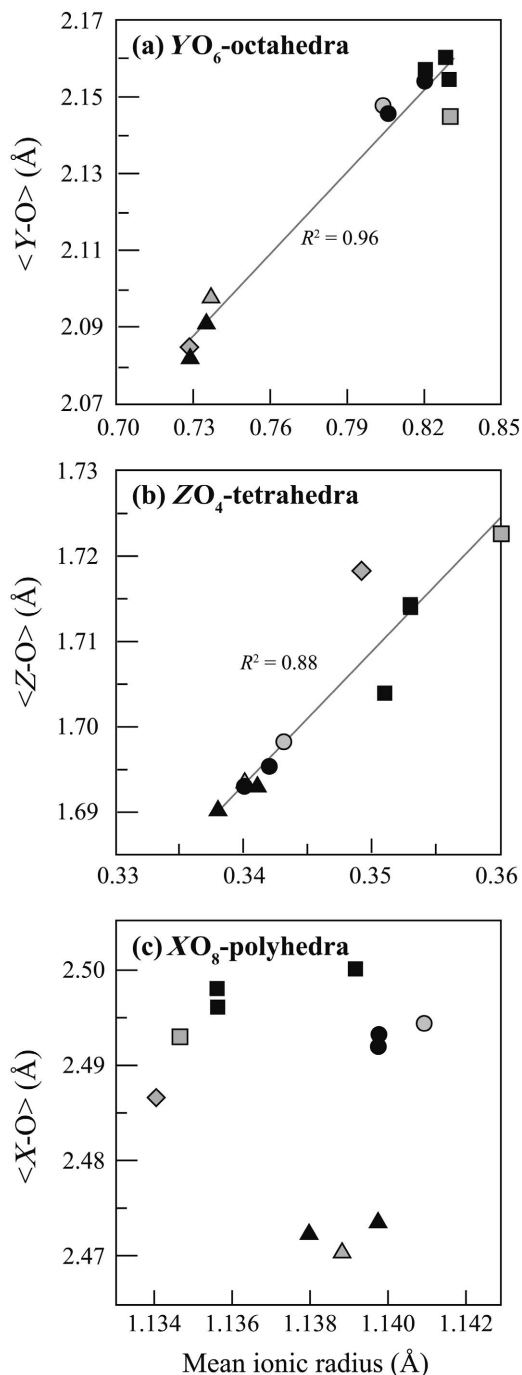

FIG. 2. Variations of (a) $<Y−O>$, (b) $<Z−O>$ and (c) $<X−O>$ as a function of mean ionic radius. Closed squares represent palenzonaite (this study), closed circles berzeliite (this study), closed circles manganberzeliite (this study), grey squares palenzonaite (Basso, 1987), grey triangles berzeliite (Hawthorne, 1976), grey diamonds schäferite (Krause *et al*., 1999) and grey circles manganberzeliite (Uwe Kolitsch, pers. comm.). Only natural compositions are plotted in this figure. The regression lines are only valid between the data points shown.
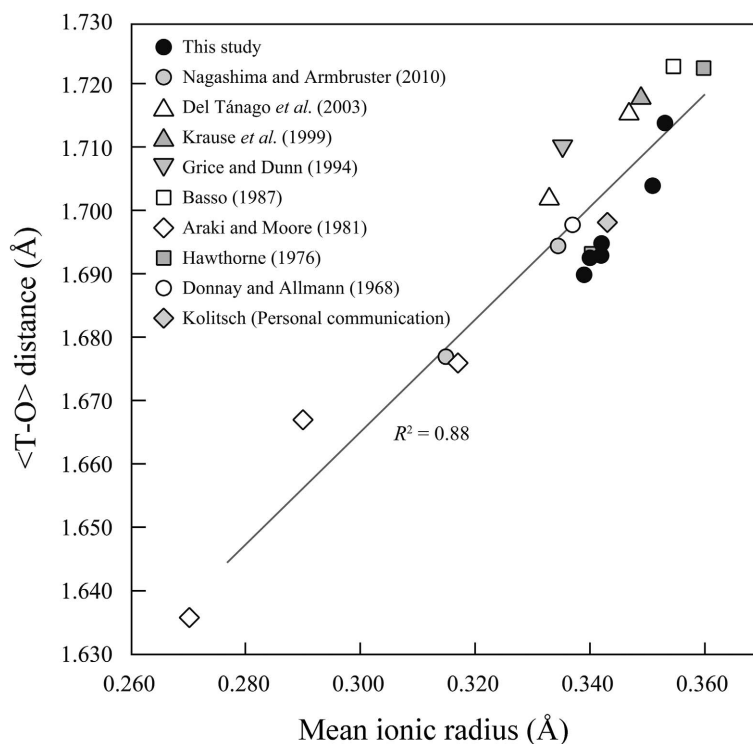
FIG. 3. Variation of $<Z-O>$ distances in none-bridging $(As^{5+}, V^{5+}, P^{5+}, Si^{4+})O_4$ tetrahedra as a function of the mean ionic radius of the $(As^{5+}, V^{5+}, P^{5+}, Si^{4+})O_4$ tetrahedron. Only natural specimens are plotted in this figure. The regression line is only valid between the data points shown.

TABLE 7. Calculated crystal structures of garnet group minerals.

Composition		$Na_3Al_2(PO_4)_3$	$Na_3Cr_2(AsO_4)_3$	$Na_3Cr_2(VO_4)_3$
Cell parameter (Å)	a	11.580	12.150	12.291
Oxygen position	x/a	0.0441	0.0387	0.0388
	y/a	0.0428	0.0480	0.0466
	z/a	0.6541	0.6517	0.6501
Selected bond distances (Å)				
Na−O (×4)		2.305	2.392	2.427
Na−O (×4)		2.477	2.520	2.563
Y−O (×6)		1.921	1.990	1.990
Shared edge		2.818	2.838	2.848
Unshared edge		2.612	2.792	2.780
Δ (shared − unshared)		0.206	0.046	0.068
$\sigma_\theta(oct)^2$*		20.65	0.99	2.12
T−O (×4)		1.535	1.693	1.720
Shared edge		2.432	2.658	2.710
Unshared edge		2.543	2.817	2.866
Δ (shared − unshared)		−0.111	−0.159	−0.156

* Angular distortion parameters are as defined by Robinson et al. (1971); $\sigma_\theta(oct)^2 = \Sigma(\theta_i - 90º)/11$ where θ_i = O−M−O angle.

TABLE 8. The O–O distances of the Y and Z sites for shared and unshared edges with the X distorted square antiprism.

	Y octahedral site			Z tetrahedral site			
	Shared edge	Unshared edge	Δ*	Shared edge	Unshared edge	Δ*	
Nat. palenzonaite	3.038(2)	3.063(2)	−0.025	2.669(2)	2.862(2)	−0.193	Molinello mine, Italy
Nat. palenzonaite	3.034(1)	3.059(1)	−0.025	2.671(1)	2.862(1)	−0.191	Gambatesa mine, Italy
Nat. palenzonaite	3.050(2)	3.059(2)	−0.009	2.653(2)	2.844(2)	−0.191	Fianel mine, Switzerland
Nat. palenzonaite	3.015(4)	3.053(4)	−0.038	2.677(4)	2.879(4)	−0.202	Basso (1987)
Syn. $NaCa_2Mn_3(VO_4)_3$	3.038(2)	3.059(2)	−0.021	2.681(2)	2.870(2)	−0.189	Nakatsuka et al. (2004a)
Nat. schäferite	2.947(2)	2.951(2)	−0.004	2.679(2)	2.867(2)	−0.188	Krause et al. (1999)
Syn. $NaCa_2Mg_3(VO_4)_3$	2.951(2)	2.956(2)	−0.005	2.6863(2)	2.871(2)	−0.185	Nakatsuka et al. (2003)
Syn. $NaCa_2Zn_3(VO_4)_3$	2.982(4)	2.996(4)	−0.014	2.674(4)	2.864(4)	−0.190	Nakatsuka et al. (2004b)
Syn. $Na_{0.9}Ca_{2.05}Co_2(VO_4)_3$	2.95(1)	2.95(1)	0.000	2.68(1)	2.87(1)	−0.190	Dukhoskaya and Mill (1974)
Nat. berzeliite	2.961(1)	2.953(1)	0.008	2.630(1)	2.822(1)	−0.192	Långban, Sweden
Nat. berzeliite	2.950(1)	2.939(1)	0.011	2.6360(9)	2.8261(9)	−0.190	Montaldo mine, Italy
Nat. berzeliite	2.967(5)	2.968(5)	−0.001	2.640(5)	2.826(5)	−0.186	Hawthorne (1976)
Nat. manganberzeliite	3.034(1)	3.036(1)	−0.002	2.637(1)	2.832(1)	−0.195	Varenche, Italy
Nat. manganberzeliite	3.044(1)	3.047(1)	−0.003	2.631(1)	2.828(1)	−0.197	Gozaisho mine, Japan
Nat. manganberzeliite	3.035(1)	3.040(1)	−0.005	2.640(1)	2.838(1)	−0.198	Uwe Kolitsch (pers. comm.)

* The Δ value is shared − unshared edge length for the appropriate site.

shared and unshared octahedral edges are listed in Table 8. Increasing the mean ionic radius of the elements at the X site has been shown to lengthen shared edges and shorten unshared edges in silicate garnets (Novak and Gibbs, 1971), but this is not observed in the arsenate and vanadate garnets in this study. In palenzonaite, the maximum difference in the refined lengths of the two octahedral edges is 0.025Å (unshared > shared). In manganberzeliite and schäferite the O−O octahedral edges are of almost equal length. The unshared octahedral edge tends to be longer than the shared edge in berzeliite, and the maximum difference is 0.011 Å (shared > unshared).

In the highly condensed garnet structure there are also shared edges between the Z tetrahedron and the distorted square X antiprism. In silicate garnets (Novak and Gibbs, 1971), the length difference between and the unshared tetrahedral edges ($4 \times$) and the shared tetrahedral edges ($2 \times$) varies between -0.257 Å (pyrope) and -0.158 Å (uvarovite). For the octahedron the difference between shared and unshared edges is considerably smaller and varies between 0.099 Å (pyrope) and -0.046 Å (goldmanite). This may indicate that tetrahedral edge distortion is not as critical for the stability of the structure. For arsenate and vanadate garnets the difference between shared and unshared tetrahedral edges varies between -0.19 and -0.20 Å (Table 8), which is within the range observed for silicate garnets (Novak and Gibbs, 1971).

Palenzonaite from manganese deposits in Liguria, the Aosta valley and the Swiss Alps and berzeliite and manganberzeliite from Långban, Varenche and Gozaisho are secondary minerals formed in veins in low-grade metamorphic facies conditions (probably <300ºC). It is inviting to assume that a less distorted arsenate or vanadate garnet structure with larger divalent cations at Y charge balanced by a mixture of Na and Ca at X would be more stable in these conditions. However, this is highly speculative and there are no reliable estimates for the crystallization temperature of minerals associated with the arsenate or vanadate garnets. Nor are there fluid inclusion studies with results that can be clearly correlated with the formation of the garnets. Matsubara (1975) noted that manganberzeliite can be formed at relatively high fO$_2$ at low temperatures, and that it is stable over a wide range of metamorphic temperature and redox conditions. In contrast, schäferite from Bellberg in the Eifel district (Krause *et al.*, 1999) is almost certainly a high temperature mineral. Synthetic schäferite (Nakatsuka *et al.*, 2003) and palenzonaite (Nakatsuka *et al.*, 2004*a*) have been synthesized by the floating zone technique from oxide melts at high temperatures. According to Ikuta and Iishi (2006), schäferite and palenzonaite were synthesized at 1100ºC and 850ºC, respectively. The preference of divalent cations for the Y site and a ratio of Ca/Na of ~2/1 at the X site (reducing structural distortion and providing charge balance) is thus a useful rule which governs the structure and composition of arsenate- and vanadate-bearing garnets, (unless they are formed at extreme pressure). There is no indication in the X-ray diffraction data of a lowering of symmetry from cubic $Ia\bar{3}d$ in spite of the close to 2/1 Ca/Na ratio at the X site.

Acknowledgements

References

Araki, T. and Moore, P.B. (1981) Dixenite, Cu^{1+}Mn$^{2+}_{14}$Fe^{3+}(OH)$_6$(As^{3+}O$_3$)$_5$(Si^{4+}O$_4$)$_2$(As^{5+}O$_4$): metallic [As$^{3+}_4$Cu^{1+}] clusters in an oxide matrix. *American Mineralogist*, **66**, 1263−1273.

Barresi, A.A., Kolitsch, U., Ciriotti, M.E., Ambrino, P., Bracco, R. and Bonacina, E. (2005) La miniera di manganese di Varenche (Aosta, Italia nord-occidentale): ardennite, arseniopleite, manganberzeliite, pirofanite, sarkinite, sursassite, thortveitite, nuovo As-analogo della metavariscite e altre specie minerali. *Micro*, 2/2005, 81−122.

Basso, R. (1987) The crystal structure of palenzonaite, a new vanadate garnet from Val Graveglia (Northern Apennines, Italy). *Neues Jahrbuch für Mineralogie Monatshefte*, **1987**, 136−144.

Bayer, G. (1965) Vanadates A$_3$B$_2$V$_3$O$_{12}$ with garnet structure. *Journal of the American Ceramic Society*, **48**, 600.

Blix, R. and Wickman, F.E. (1959) A contribution to the knowledge of the mineral berzeliite. *Arkiv for Kemi Mineralogi Och Geologi*, **2**, 417−424.

Brugger, J. (1995) Mineralogy of the iron-manganese deposit of Fianel, Ferrera valley, Graubünden.

Schweizerische Mineralogische Petrographische Mitteilungen, **75**, 296−297.

Brugger, J. and Berlepsch P. (1996) Description and crystal structure of fianelite, $Mn_2V(V,As)O_7·2H_2O$, a new mineral from Fianel, Val Ferrera, Graubünden, Switzerland. *American Mineralogist*, **81**, 1270−1276.

Bruker (1999) *SMART and SAINT-Plus. Versions 6.01*. Bruker AXS Inc., Madison, Wisconsin, USA.

Brunet, F., Bonneau, V. and Irifune, T. (2006) Complete solid-solution between $Na_3Al_2(PO_4)_3$ and $Mg_3Al_2(SiO_4)_3$ garnet at high pressure. *American Mineralogist*, **91**, 211−215.

Del Tánago, J.G., La Iglesia, Á., Rius, J. and Santín, S.F. (2003) Calderonite, a new lead-iron vanadate of the brackebuschite group. *American Mineralogist*, **88**, 1703−1708.

Donnay, G. and Allmann, R. (1968) Si_3O_{10} groups in the crystal structure of ardennite. *Acta Crystallographica*, **B24**, 845−855.

Dukhovskaya, E.L. and Mill, B.V. (1974) Refinement of the crystal structure of vanadium garnet $Na_{0.9}Ca_{2.05}Co_2V_3O_{12}$. *Soviet Physics Crystallography*, **19**, 47−49.

Frondel, C. and Ito, J. (1963) Manganberzeliite from Franklin, New Jersey. *American Mineralogist*, **48**, 663−664.

Grice, J.D. and Dunn, P.J. (1994) Johninnesite: crystal-structure determination and its relationship to other arsenosilicates. *American Mineralogist*, **79**, 991−995.

Hawthorne, F.C. (1976) Refinement of the crystal structure of berzeliite. *Acta Crystallographica*, **B32**, 1581−1583.

Hawthorne, F.C. (1981) Some systematics of the garnet structure. *Journal of Solid State Chemistry*, **37**, 157−164.

Holtstam, D. and Langhof, J. (editors) (1999) *Långban: the Mines, their Minerals, Geology and Explorers*. Swedish Museum of Natural History, Raset Förlag, Stockholm, 215 pp.

Iishi, K. and Ikuta, Y. (2006) Isomorphous substitutions in vanadate garnets. *Neues Jahrbuch für Mineralogie, Abhandlungen*, **182**, 157−163.

Ito, J. (1968) Synthesis of the berzeliite $(Ca_2NaMg_2As_3O_{12})$-manganese berzeliite $(Ca_2NaMn_2As_3O_{12})$ series (arsenate garnet). *American Mineralogist*, **53**, 316−319.

Krause, W., Blaβ, G. and Effenberger, H. (1999) Schäferite, a new vanadium garnet from the Bellberg volcano, Eifel, Germany. *Neues Jahrbuch für Mineralogie, Monatshefte*, **1999**, 123−134.

Kolitsch, U. (2008) The crystal structure of a new Ca-Na-Mn^{3+}-arsenate from a small metamorphic Mn deposit in Italy. Abstract of the 18th Annual V. M. Goldschmidt Conference, Vancouver, Canada, *Geochimica et Cosmochimica Acta*, **72**, Special Supplement 12S, A487.

Matsubara, S. (1975) Manganberzeliite from the Gozaisho mine, Fukushima Prefecture, Japan. *Journal of the Mineralogical Society of Japan*, **12**, 238−52, [in Japanese].

Momma, K. and Izumi, F. (2008) *VESTA*: a three-dimensional visualization system for electronic and structural analysis. *Journal of Applied Crystallography*, **41**, 653−658.

Nagashima, M. and Armbruster, T. (2010) Ardennite, tiragalloite and medaite: structural control of (As^{5+}, V^{5+}, Si^{4+})O_4 tetrahedra in silicates. *Mineralogical Magazine*, **74**, 55−71.

Nakatsuka, A., Ikuta, Y., Yoshiasa, A. and Iishi, K. (2003) Vanadate garnet, $Ca_2NaMg_2V_3O_{12}$. *Acta Crystallographica*, **C59**, i133−i135.

Nakatsuka, A., Ikuta, Y., Yoshiasa, A. and Iishi, K. (2004a) The crystal structure of synthetic palenzonaite $Ca_2NaMn_2V_3O_{12}$. Pp. 631−634 in *Applied Mineralogy: Developments in Science and Technology* (M. Pecchio, F.R.D. Andrade, L.Z. D'Agostino, H. Kahn, L.M. Sant'Agostino and M.M.M.L. Tassinari, editors). Proceedings of the International Congress on Applied Mineralogy, **2**. ICAM-BR, Sãn Paulo, Brazil.

Nakatsuka, A., Ikuta, Y., Yoshiasa, A., Iishi, K. (2004b) Single crystal X-ray diffraction study of the vanadate garnet $Ca_2NaZn_2V_3O_{12}$. *Materials Research Bulletin*, **39**, 949−956.

Novak, G.A. and Gibbs, G.V. (1971) The crystal chemistry of the silicate garnets. *American Mineralogist*, **56**, 791−825.

Piccoli, G.C., Kolitsch, U., Blass, G. and Ciriotti, M.E. (2007) Berzeliite di Montaldo di Mondov: prima segnalazione italiana. *Micro*, 1/2007, 49−54.

Robinson, K., Gibbs, G.V. and Ribbe, P.H. (1971) Quadratic elongation: a quantitative measure of distortion in coordination polyhedra. *Science*, **172**, 567−570.

Roth, P. and Meisser, N. (2011) I minerali dell'Alpe Tanatz. *Rivista Mineralogica Italiana*, **35**, 90−98.

Schwarz, H. and Schmidt, L. (1972) Neue Verbindungen mit Granatstruktur. IV. Arsenate des Typs $\{Na_3\}[M_2^{III}](As_3)O_{12}$. *Zeitschrift für Anorganische und Allgemeine Chemie*, **387**, 31−42.

Schwarz. H. and Schmidt, L. (1975) Neue Verbindungen mit Granatstruktur. VI. Vanadate. *Zeitschrift für Anorganische und Allgemeine Chemie*, **413**, 150−164.

Shannon, R.D. (1976) Revised effective ionic radii and systematic studies of interatomic distances in halides and chalcogenides. *Acta Crystallographica*, **A32**, 751−767.

Sheldrick, G.M. (1996) *SADABS*. University of Göttingen, Göttingen, Germany.

Sheldrick, G.M. (2008) A short history of *SHELX*. *Acta Crystallographica*, **A64**, 112−122.

Thilo, E. (1941) Über die Isotypie zwichen Phosphaten der allgemeinen Zusammensetzung $(Me_1)_3(Me_2)_2[PO_4]_3$ und den Silikaten der Granatgruppe. *Naturwissenschaften*, **29**, 239.